Intrinsic reactivity analysis of soot removal in LNT-catalysts

Marina Cortés-Reyes, Concepción Herrera, María Ángeles Larrubia, Luis J. Alemany [*]

Departamento de Ingeniería Química, Facultad de Ciencias, Campus de Teatinos, Universidad de Málaga, Málaga E-29071, Spain

ARTICLE INFO

ABSTRACT

The soot removal process in presence of a series of LNT-catalysts, and different reaction atmospheres, has been studied, using thermogravimetric analysis coupled to mass spectrometry (TG-MS) time-resolved experiments. Kinetic parameters have been estimated, using a distribution function of activation energy: where the frequency factor was correlated approximately with the activation energies which enable the decoupling of the processes involved in the regeneration by soot removal over those synthesized catalysts. It was found that soot removal is a sequential process that is strongly dependent on the formulation and surface structure of the catalyst and atmosphere of reaction. K-containing LNT catalysts showed a high activity in the soot removal process by gasification ($Ea \approx 70$–$90 kJ\,mol^{-1}$), promoted by surface hydroxylated centers, decreasing the ignition temperature in oxygen atmosphere. $NO + O_2$ atmosphere, more oxidizing than O_2, provokes in addition a reduction in the soot removal temperature due to a direct reaction between soot and NO_2 (gas) and/or the adsorbed NO_x onto the catalyst surface.

© 2016 Elsevier B.V. All rights reserved.

1. Introduction

In the last decades the sales of vehicles with Diesel engines have been increasing due to its fuel efficiency, reliability and durability [1–5]. The main drawback of this type of vehicle is the emission of contaminants into the atmosphere, such as nitrogen oxides (NO_x) and particulate matter (soot), which are responsible for serious health and environmental problems [2,6–13]. Reducing these emissions below the limits imposed by the regulations requires the use of catalytic after-treatment technologies that allow the elimination of the maximum possible amount of NO_x and soot [14].

In terms of nitrogen oxides removal, there are two widely used technologies because of their efficacy and selectivity: selective catalytic reduction (SCR) and NO_x storage and reduction (NSR) [5]. SCR technology is based on the mineralization of NO_x to N_2 and water by reaction with NH_3 [14,15]. This system requires the injection of an external reducing agent, which makes its implementation in mobile sources difficult. However, currently, the coupling between the SCR and NSR technologies is being widely studied to solve this drawback [16–19]. At present, the NSR technique is the most efficient in removing nitrogen oxides from the diesel exhaust gases [20,21]. It consists of alternating cyclic lean-rich conditions. So that, when oxygen is in excess (lean fuel mixture), the NO_x are retained and partially stored as nitrate and nitrite on the catalyst surface. These

species react in the following phase (fuel rich) producing nitrogen and water [1,2,22–24].

Among the NSR catalysts, Co-based oxide catalysts such as mixed oxides, perovskites and hydrotalcite-derived oxides have attracted much attention because of their excellent catalytic oxidation ability [2]. However, standard NSR catalysts consist of precious metals and alkaline/alkaline-earth metal oxides, typically platinum and barium, respectively, dispersed on metal oxide supports such as alumina [23].

There are two ways to remove the particulate matter (PM) effectively. One of them consists of using Diesel Oxidation Catalyst (DOC), whose main function is to selectively oxidize CO and a wide range of hydrocarbons that are part of the soot. This type of system is located just downstream of the engine and is usually a cordierite support structure through which exhaust gas flows. It is covered with a high surface area washcoat where the active phase is supported. Catalysts based on cobalt, iron or manganese oxides with noble metals such as platinum or palladium are the most common [5,14,25]. The most widely used system in the PM removal is the Diesel Particulate Filter (DPF). This filter consists of a monolithic device with porous walls, through which the gas from the engine goes across, while the particles are retained [4,26–30]. To prevent these particles hindering the circulation of gas, when the pressure rises to a certain level, it sends a small amount of fuel that causes an increase in temperature and burns the entire amount of particles deposited on the filter. So, it is completely regenerated and can continue working in optimal conditions. A wide range of catalysts has been studied for this purpose, such as single and mixed metal oxides

Table 1
Formulation of studied catalysts.

Catalysts		Pt(wt.%)	Ba(wt.%)	K(wt.%)	Al$_2$O$_3$(wt.%)
0.4Pt-4Ba/γ-Al$_2$O$_3$	PtBa/Al$_2$O$_3$	2	20	–	78
0.4Pt-16 K/γ-Al$_2$O$_3$	PtK/Al$_2$O$_3$	2	–	20	78
0.4Pt-3.5Ba-1.5 K/γ-Al$_2$O$_3$	PtBaK/Al$_2$O$_3$	2	18	2	78

or perovskite- and spinel-type oxides [14,30–33]. Some authors believe that the addition of potassium combined with platinum to the catalyst formulations is one of the most promising options for soot oxidation [7,14].

The most used technology for this purpose is known as Diesel Particulate-NO$_x$ reduction (DPNR) developed by Toyota [8,9,14,23,34]. This technique consists of using a porous ceramic filter coated with a catalytic layer composed of a high surface area support (such as a gamma Al$_2$O$_3$), a noble metal (Pt) and an alkali or alkaline-earth metal oxide, which present a high NO$_x$ storage capacity. The procedure is similar to NSR technology as it works in cyclical conditions, alternating fuel-lean phases, during which the nitrogen oxides produced by the engine are adsorbed on the storage element, with rich fuel phases in which the nitrates are reduced to nitrogen, as was explained above [8]. The stored nitrates decrease the soot combustion temperature. However, it must be taken into account that there is a minimum in the combustion temperature, which cannot be reduced by the use of catalysts, since it depends on the soot characteristics [35].

Although other catalysts have been proposed for this aim, such as precious metals [13,23,36], zeolites [37] perovskite-related oxides [38]; spinel phases [39] and hydrotalcite-derived compounds modified by transition metal ions [10,40], which exhibit excellent properties, the standard NSR catalyst, Pt-Ba/Al$_2$O$_3$ is capable of storing NO$_x$ and oxidizing soot simultaneously, as it works in the same conditions. Nevertheless, there is a decrease in the storage capacity due to the formation of Ba-carbonates species [41]. Therefore, new improved systems are proposed, including potassium, so that the NO$_x$ removal is produced on the alkaline-earth, while the soot oxidation process is associated with the alkali metal [42]. The high activity of potassium in the soot oxidation reaction is due to the high mobility of some compounds of potassium, which improves the contact between catalyst-soot [6].

The role played by the alkali metals and alkaline-earths metals in removing soot is under investigation. Castoldi et al. [31] indicated the beneficial effect of the addition of these metals in the catalyst formulation for soot removal, both in the catalyst as in the particulate filter.

In order to improve the catalyst formulation it is necessary to understand the behaviour of each of its elements in the particulate matter removal process. For this reason, the mechanism of soot oxidation with and without catalyst has been extensively reported in literature [43,44]. To study this process thermogravimetric analysis (TGA) has been generally used since it allows working with gas-solid reactions and distinguishing between competing models [32,45,46]. Besides the type of analysis, the physical contact between the soot and catalyst is another factor to consider, because the soot combustion in air on a catalyst proceeds via a three-phase reaction. Tight contact mode is the most used method to study this mechanism; although it does not represent the real situation, it makes possible the study of the intrinsic catalytic combustion of soot [6,32,36,40,46].

In the absence of any catalyst and in the presence of air López-Fonseca et al. [47] postulated that the combustion occurs through a single-rate process, which involves penetration of oxygen and subsequent combustion inside the porous structure. This reaction could be via dissociative chemisorption of oxygen, which leads to

Table 2
Pt$^\circ$/Pt$_{ox}$ ratio for different catalyst.

	Pt/Al$_2$O$_3$	PtBa/Al$_2$O$_3$	PtK/Al$_2$O$_3$	PtBaK/Al$_2$O$_3$
Pt^0/Pt$_{ox}$	1.2	1.8	0.6	1.8

oxygen radicals that subsequently form (unable) surface oxygen complexes that would decompose forming CO and CO$_2$ [43,48].

The mechanism of soot removal in other oxidizing atmospheres has also been proposed [44,49]. When NO$_2$ and O$_2$ are both present in the gas mixture, it is supposed that the oxygenated carbon complexes are firstly formed from the reaction between soot and NO$_2$, enhancing the soot oxidation at lower temperatures [23,44,49].

The mechanism of the metal-catalysed reaction could be similar to the non-catalytic reaction [1,43]. It has been shown that the presence of soot decreases the NO$_x$ storage activity of the catalysts, due to an interaction between soot and the stored NO$_x$ that provides an additional route for oxidation of the carbonaceous material [4,9,23,34,41,48].

The aim of this work is to develop a methodology to be applicable to the analysis of complex reactions and in particular to deduce the intrinsic removal mechanism of soot in the presence of different catalysts and reaction atmospheres in order to clarify the behavior of the alkaline and alkaline-earth in the overall process; by kinetic approach of the multiple reactions taking account of the variation of frequency factor.

2. Experimental

2.1. Catalysts preparation and characterization

A series of catalysts, model and improved, prepared by incipient wetness impregnation has been studied; the protocol has been detailed in previous works [1,42,50] and it consists of the impregnation of γ-Al$_2$O$_3$ (Sasol) with the platinum precursor, Pt(NH$_3$)$_2$(NO$_2$)$_2$ (Pt content 3.4 wt.%, Aldrich Chemical) and subsequently, the barium and/or potassium precursor (Ba(CH$_3$COO)$_2$, Merck), (CH$_3$COOK, Fluka) with intermediate and final calcination in air. The metal loading expressed as formal surface atomic density (atoms per nanometre square, at/nm^2) and the catalyst weight percentage composition are summarized in Table 1. To study the intrinsic kinetic parameters of the catalytic removal of particulate matter, 10% soot from Degussa Printex U (its composition consists of 97.17, 1.16, 0.19 and 0.31 wt.% of C, H, N and S, respectively) was added using the tight contact method [6]. The detailed properties of Printex U (Degussa) are well described in the literature [44,51]. Furthermore, a sample of bare soot was prepared, constituted by 10% soot in quartz.

Synthesized catalysts have been characterized by several techniques such as X-ray Diffraction (XRD), X-ray Photoelectron Spectroscopy (XPS) and High Resolution Transmission Electron Microscopy (HRTEM). These data have been reported in previous works [42]. Although, the results obtained from XPS are interesting because of their relation with the reactivity. So, this characterization technique and results are detailed here. The XPS spectra were obtained by using a Physical Electronic 5700 spectrometer with Mg Kα X-ray source and hemispherical electron analyzer. The carbon C1s peak at 284.8 eV was used as internal standard for
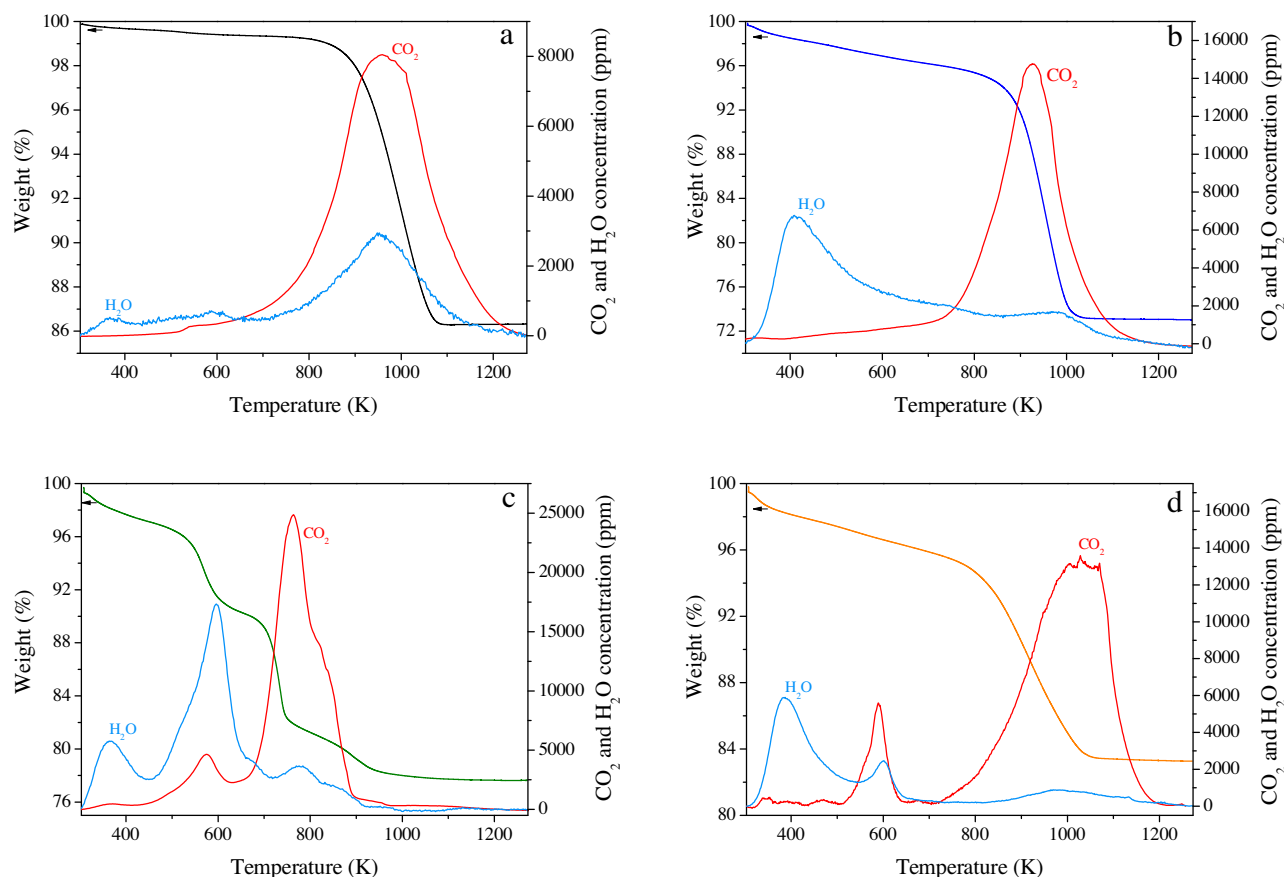
Fig. 1. Weight loss and products distribution vs. temperature in the presence of 3% of O_2 in He for (a) soot, (b) PtBa/Al$_2$O$_3$, (c) PtK/Al$_2$O$_3$ and (d) PtBaK/Al$_2$O$_3$.

determining peak positions within ± 0.2 eV accuracy. All deconvolutions of experimental curves were done with Gaussian–Lorenzian line fitting of varying proportions (60–80%).

2.2. Catalytic study

Thermogravimetric analysis (TG-MS)

Thermogravimetric analysis (TG-DSC) was employed for the kinetic study of the intrinsic reactivity of the synthetized catalysts in the soot removal process. The TG/DSC data was acquired using a SDT Q600 thermobalance from T.A. Instrument. The sample was loaded into the chamber and when the weight of the sample reached a constant value in He atmosphere, it was heated from room temperature to 1273 K at a rate of 10 K min^{-1} in the atmosphere of NO/O$_2$ (1000 ppm of NO + 3% O$_2$ in He flow) or O$_2$ (3% of O$_2$ in He flow), maintaining a total gas flow rate of 100 ml min^{-1} (which was large enough to neglect the mass transfer resistance of the particle) for 10 mg of sample (GSHV = 2×10^4 h^{-1} STP). No significant differences were recorded in TG-profiles indicating that intraparticle resistance is negligible for the particles smaller than 0.9 mm in diameter. The gas composition at the outlet of the thermobalance was temporally analysed on line by mass spectrometry with a Pfeiffer Prisma^{TM} Quadrupole Mass Spectrometer QMS 200.

3. Results and discussion

3.1. Catalysts characterization

These catalysts have been characterized in previous works [1,42,50]. However, the Pt oxidation state data obtained from XPS results justify the cooperation between the alkali element and Pt

[1,52] and are relevant for this study. So, in Table 2 the Pt$^\circ$/Pt$_{ox}$ ratio (Pt$_{ox}$ = Pt^{2+} + Pt^{4+}) for the studied catalysts is shown. Pt/Al$_2$O$_3$ has also been included for comparison. This relationship has been obtained from the deconvolution of the signal from Pt4d$_{5/2}$ region, which provides three bands with binding energies, similar for all the catalysts and ca. 314, 317 and 320 eV, corresponding to Pt$^\circ$, Pt^{2+} and Pt^{4+}, respectively. It can be observed that Ba-containing catalysts show the highest Pt$^\circ$/Pt$_{ox}$, which suggests an improved Pt-alkali cooperation, resulting in excellent performance in removing NO$_x$, as is shown in bibliography [1,8,31,52]. PtK/Al$_2$O$_3$ catalyst, whose Pt$^\circ$/Pt$_{ox}$ ratio is lower than 1, presents a lower NO$_x$ removal capacity. It has been proved that potassium limits the catalyst reducibility [1]. Despite these drawbacks, the behaviour of K in the formulation due to its high reactivity in the soot oxidation was reported earlier [1,3,8,11,31,53]. So, the addition of an optimized potassium loading in the formulation was justified for its efficacy in removing soot and the N$_2$-selectivity increase in the regeneration step [1,42,50].

3.2. Reactivity study

In order to better understand the soot removal pathway and the estimation of kinetic parameters; TG-MS curves were performed in different oxidation atmospheres measured at a constant heating rate (10 K min^{-1}) and obtained under chemical regime; i.e out of mass transfer limitations. The TG curves must be obtained under chemical regime to evaluate f(E) (distribution function of activation energy); so the mass transfer resistance for the current particle size (<1 mm in diameter) was negligible at the flow rate of 100 ml min^{-1} (STP). These experiments are completely repetitive and we ensure that working conditions are outside the diffusional limits.
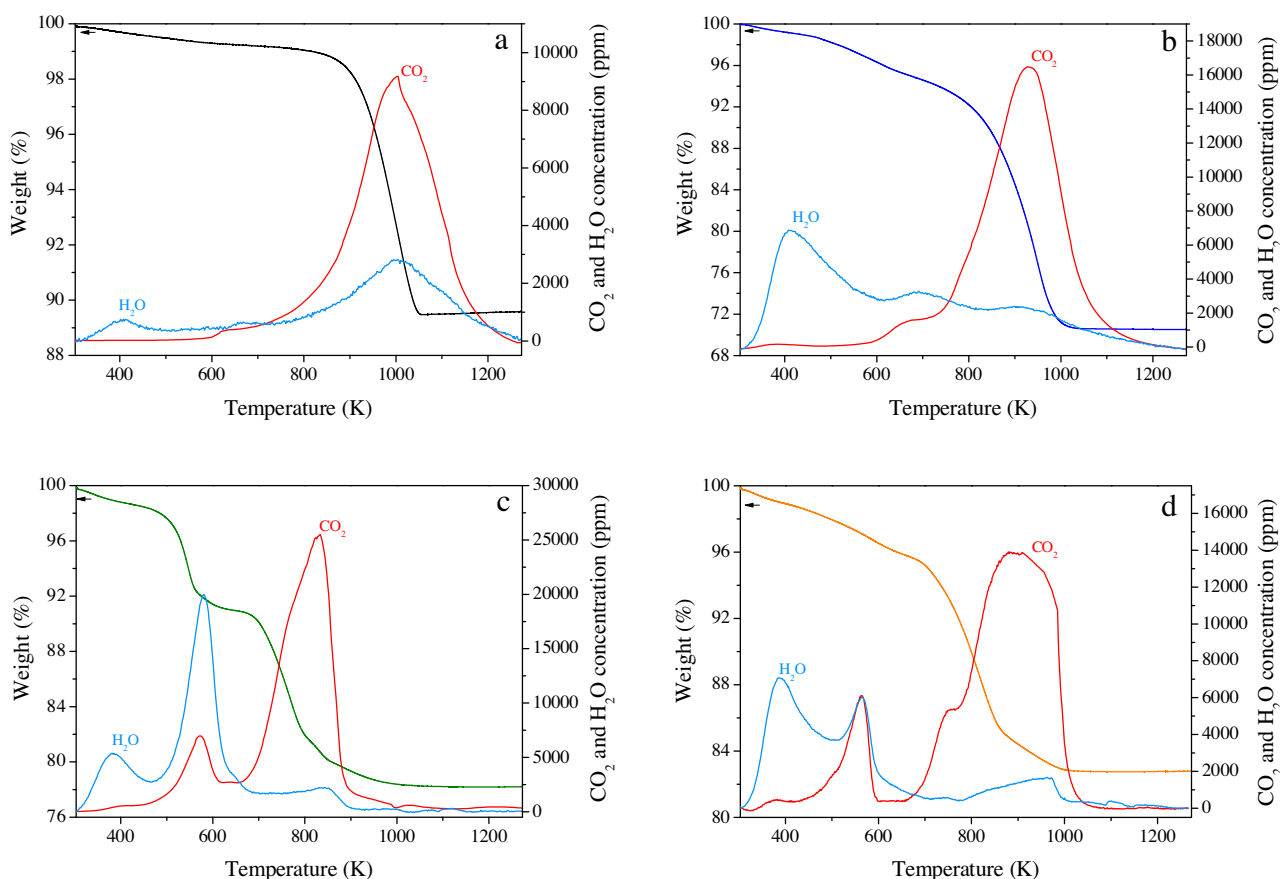
Fig. 2. Weight loss and products distribution vs. the temperature in the presence of 1000 ppm of NO and 3% of O_2 in He for (a) soot, (b) $PtBa/Al_2O_3$, (c) PtK/Al_2O_3 and (d) $PtBaK/Al_2O_3$.

Additionally, the contact conditions and the size of soot particles are variables which was initially taken into consideration and no influence was noticed in the experiments since we are working with high carrier gas flow.

The weight loss of soot in the presence of different catalysts in atmosphere of O_2 (3% He-balance) are shown in Fig. 1, together with the concentration of water and CO_2 measured by MS. The profile obtained for soot (free-catalyst) is included as well. The weight loss observed for soot, (Fig. 1a) in oxygen atmosphere, is close to 10% of the initial weight and it was produced in a single step and registered in the range between 873 and 1073 K. However, the TG profiles for the soot removal in O_2-atmosphere over alkaline-modified Pt alumina-supported catalysts (LNT improved catalysts) showed that the soot removal occurs in a different way even at lower temperatures. In presence of $PtBa/Al_2O_3$, with a standard formulation for LNT catalysts, the soot removal also takes place in a single step but with a higher weight loss rate and in a slightly lower temperature range than soot free-catalyst, indicating that is an activated process.

For PtK/Al_2O_3 where the Ba was substituted by K, with a metal loading for the same surface coverage, the TG curve registered is completely different; in which three steps for the soot-removal process can be clearly differentiated. A region between 473 and 623 K with a loss of 7% was observed related to the dehydration of chemisorbed water. A second step, from 623 to 773 K where 10% of soot is eliminated and CO_2 and H_2O formation were registered. Finally, a third temperature window at higher temperature with a weight loss of 4% associated with the removal of the rest of the soot, by combustion, possibly with less contact with the catalyst. The soot removal process over $PtBaK/Al_2O_3$ occurs in a wider temperature range, between 673 and 1073 K and the weight loss

corresponds to 11% of the total. An intermediate behaviour between $PtBa/Al_2O_3$ and PtK/Al_2O_3, was found for the trimetallic catalyst; although, apparently it is closer to Ba-containing catalyst due to the similar relative load of this element in the formulation. So that the expected reactivity in the catalytic soot oxidation depends on the electropositive character of the metal added to the catalyst formulation and the surface species. It is evidenced that the presence of K or Ba oxides modifies the CO_2 production with respect to the uncatalyzed soot oxidation and the H_2O released is more dependent for the K-containing catalysts.

TG-curves in atmosphere of $NO + O_2$ and the CO_2 and H_2O distribution profiles are shown in Fig. 2. The uncatalyzed soot removal presents a weight loss of 10% and the temperature range is narrower than was observed in O_2-atmosphere, due to a more oxidizing environment. For the standard LNT-catalyst formulation ($PtBa/Al_2O_3$, Fig. 2b) the soot removal occurs in a single step between 773 and 1073 K with a weight-loss close to 22%, associated with the elimination of the particulate matter and a further decarbonation of the catalyst. This process is activated and the temperature interval in which the soot combustion takes place is consistent with data reported by other authors [15]. For PtK/Al_2O_3 the TG profile is absolutely different, in which three consecutive weight losses were registered and associated with a sequential soot elimination process; with an additional partial dehydration by chemisorbed water between 473 and 623 K with a weight loss of 7%. The three sequential steps are detected at 623–773 K, 773–873 K and 873–1023 K with weight losses of 9, 2.5 y 2%, respectively. Contrary to what was registered for the uncatalyzed and over $PtBa/Al_2O_3$ catalyst, the MS-signals for H_2O and CO_2 in the case of K-containing catalyst is also different even in $NO + O_2$ atmosphere. So, four non-symmetrical

signals for the water evolution were registered and a peak close to 600 K and an asymmetrical signal between 700 and 900 K in the CO_2 profile. The TG-curve obtained over $PtBaK/Al_2O_3$ was intermediate to those observed for the PtBa and PtK model catalysts, showed sequential steps although it is closer to the catalyst that incorporates the alkaline-earth metal. The mass lost strongly increased in presence of $NO + O_2$ although the total burn-off associated with ash, practically remained unaffected. In addition, the soot elimination occurs in a lower temperature range compared with the same experiment in absence of NO, due to a greater oxidizing environment [49]. For Pt-containing catalysts the effect of Pt on catalytic oxidation of soot, facilitating the NO-oxidation, has been discussed so far in the literature. NO_2 formation is enhanced by Pt and transported via the gas phase over soot particles, oxidizing carbon while being reduced to NO itself [54]. NO_2 is known to oxidize soot at lower temperature than O_2, being a stronger oxidant [44,49,50]. However, some form of cooperative effect exists, promoted by the alkali or alkaline earth in the LNT catalysts that modifies the curves and the profiles in the soot removal process. All samples exhibit a slight weight loss up to 623 K attributed to the desorption of water adsorbed on soot particle besides of the chemisorbed water depending of chemical nature of catalysts [54]. The peaks registered at higher temperatures, above 973 K, are associated with soot combustion although slightly shifted, in agreement with the reported earlier by Castoldi et al. [31], by the presence of either alkaline or the alkaline-earth oxide species. However, intermediate signals also improved the soot removal, and must be associated to other contributions that are related to the formulation of catalysts and improves the overall process of the elimination of carbon particles.

The TG-profiles and the gas-product distribution observed suggest that there are activated processes whose frequency of occurrence depends on the characteristics of the catalyst and the reaction atmosphere. The analysis of complex reactions to deduce the intrinsic removal mechanism of soot in the presence of different catalysts and reaction atmospheres has been approached through kinetic data, taking account the variation of frequency factor of the single processes. So, the decoupling of the complex reactions allows the establishment of an explained route of the soot removal process in the presence of LNT-catalysts. The kinetic was analyzed on the basis of a model that the soot-removal reaction consists of a network of first-order reactions each of which has different activation energy and a frequency factor. The frequency factors were approximately correlated by a function of the activation energy. The different activation energies were represented by a distribution curve obtained from the TG-curves measured at a constant heating rate. The weight loss during removal process, in different environments, was predicted by using the curve determined by the proposed method.

It is assumed that the soot removal process takes place through a series of irreversible, independent and parallel first-order reactions. The differences in the reaction rates are represented by the activation energy and the frequency factor values. So, the weight loss of soot elimination of the i-th adsorbed species is represented by:

$$-\frac{dm_i}{dt} = k_{0_i} \times e^{-E_i/RT} \times m_i \tag{1}$$

where m_i (mg) is the mass-weight, E_i and k_{0i} are, respectively, the activation energy (kJ·mol^{-1}) and the frequency factor (s^{-1}) if the rate equation of the Arrhenius type is assumed. Anthony et al. [53] analyzed the fast pyrolysis of coal based on a model which assumes that the pyrolysis consists of a large number of first-order independent reactions, from the Vand originally derived model [54] for analyzing the irreversible change in the resistance of metallic films

prepared by evaporation. According to this model the unconverted fraction $q(t)$ is given as a function of time and temperature as:

$$q(t) = \frac{m(t)}{m_o} = \int_0^\infty exp\left[-k_o \int_0^t e^{-E/RT} dt\right] f(E)\, dE \tag{2}$$

where $f(E)$ is the distribution function of activation energy defined so as to satisfy

$$\int_0^\infty f(E)\, dE = 1 \tag{3}$$

The value of the frequency factor is not constant and is related to the activation energy, based on a well-known experimental fact that the frequency factor increases with the increase of activation energy. The relation between them, given by Eq. (4), is known as "compensation effect" in the field of chemical reaction kinetics [55]:

$$k_o = \alpha \times e^{\beta E} \tag{4}$$

where α and β are positives constants determined experimentally, which vary depending on the nature of the process. In previous experiments about the decomposition of organic adsorbed on these LNT-catalysts were found that the frequency factor (k_0) increases with the activation energy and the following equation (α and β) holds approximately:

$$k_o = \alpha \times e^{\beta E}; k_o = 10^7 \times e^{0.043E}$$

these data provides activation energy values that are within the ranges given in literature using other routes for estimation, such as *Kissenger-Akahira-Sunose* isoconversional methods, *Coats-Redfern* model-fitting method or the equation proposed by *Brukh* and *Mitra* [29,32,33,46,47,49,56].

Substituting Eq. (4) in Eq. (2) it is obtained the following expression

$$q(t) = \int_0^\infty exp\left[-\alpha \times e^{\beta E} \int_0^t e^{-E/RT} dt\right] f(E)\, dE \tag{5}$$

The Eq. (5) indicates that the weight-loss can be estimated when the relation between temperature and time are given, and α and β and $f(E)$ are predetermined. The distribution curve of activation energy, $f(E)$ was determined by the analysis of the thermogravimetric curve at a constant heat rate (a) and the Eq. (5) is approximately rewritten to

$$q(T) \cong \int_0^\infty \Phi(E, T) f(E)\, dE \tag{6}$$

where $\Phi(E, T)$, related to the temperature and the activation energy and consider the Poisson approximation, can be approximated by

$$\Phi(E, T) \cong exp\left[-\frac{\alpha e^{\beta E} T}{a} \times \frac{e^{-E/RT}}{E/RT}\right] \tag{7}$$

By examining the change of $\Phi(E, T)$ with respect to E at fixed temperatures, $\Phi(E, T)$ was found to be approximated by the tangent line at the inflection point of $\Phi(E, T)$. Based on this approximation $f(E)$ is formulated approximately as

$$f(\bar{E}) = -\frac{(1+S)^2}{R\left[P\left(P + M/P\right)\left(e/2 + S\right) + P(2S - P)\right]} \times \frac{dq}{dT} \tag{8}$$

where P, S, $\bar{E}$ and M are related to temperature (T), respectively, by the following equations.
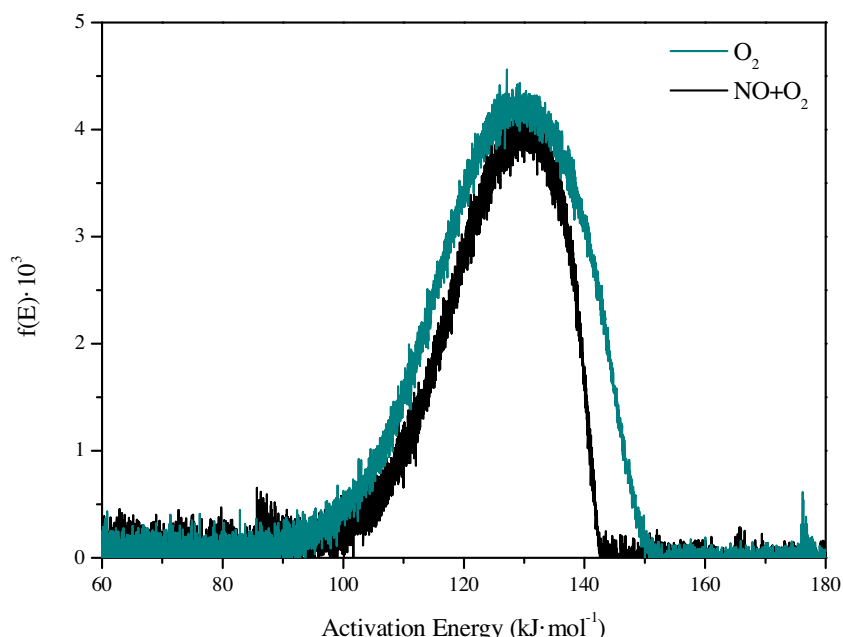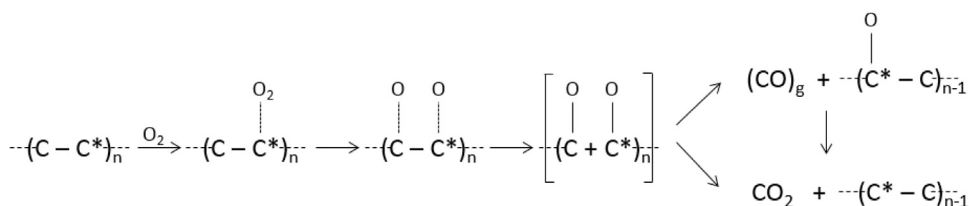
$$P = E_{in}/RT \tag{9}$$

Fig. 3. Distribution functions of activation energy for the uncatalyzed soot elimination in different atmospheres.

Scheme 1. Mechanism of uncatalyzed soot combustion under O_2 atmosphere.

$$S = P - \beta E_{in} \quad (10)$$

$$\bar{E} = \left[(2S + e) / 2(S + 1) \right] E_{in} \quad (11)$$

$$M = P(2 + P) / (1 + S) \quad (12)$$

where E_{in} is the activation energy at the inflection point at Eq. (7), and is approximately related to T by

$$\frac{aE_{in}}{\alpha e^{\beta E_{in}} RT^2} \cong e^{-E_{in}/RT} \quad (13)$$
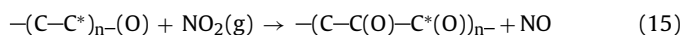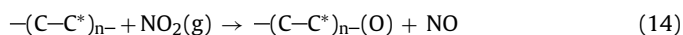
All terms of the right side of Eq. (8) can be calculated beforehand for select T values by the Eqs. (9)–(12). The differential term in right side of Eq. (8) by differentiating numerically the TG-curve at a constant heating rate.

The function of distribution of activation energy obtained for the uncatalyzed soot removal in O_2 and $NO + O_2$ atmospheres are shown in Fig. 3. In presence of oxygen, the distribution function is a quasi-symmetric unimodal Gaussian type curve with a maximum frequency value for the activation energy close to 130 kJ mol^{-1}. Where CO_2 was the main product detected in the temperature range between 823 and 1123 K. This value is in agreement with other values of activation energy reported in bibliography for particulate matter combustion reactions, when soot samples with similar characteristics to Printex U are used. Although, the activation energy values could vary between 130 and 160 kJ mol^{-1}, depending on the heterogeneity of the surface and structural properties of soot [29,33,48,54,57]. It is generally accepted that the soot combustion follows a mechanism based on surface nucleation with subsequent movement of the resulting surface, which is consistent with the penetration of oxygen through the porous structure of
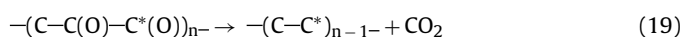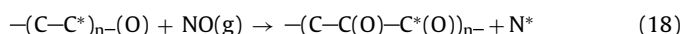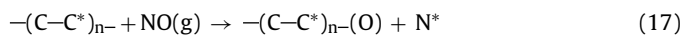
the solid sample and finally the spheres reduce in size until total combustion (Scheme 1) where C* is an available carbon site to be oxidized.

For the uncatalyzed soot elimination in $NO + O_2$ atmosphere, the function of distribution is an asymmetric and narrower curve with a single and relative maximum close to 130 kJ mol^{-1}. In which an increase in the NO signal is detected by MS in the temperature range between 823 and 923 K and CO_2 was the main product registered in a wider temperature range between 833 and 1023 K.

It is evident that the influence of NO_x of the gas phase improves the oxidation of surface; but two possible mechanisms, depending on the main present species NO_2 or NO, are possible. In agreement with the MS data for the products distribution, where NO detection and CO_2 formation were registered with a progressive shortening of carbon chain and the data previously reported [34,49] for the NO_2, the following reactions (Eqs. (14)–(16)) could represent the route of soot removal for the uncatalyzed process

$$-(C-C^*)_{n-} + NO_2(g) \rightarrow -(C-C^*)_{n}-(O) + NO \quad (14)$$

$$-(C-C^*)_{n}-(O) + NO_2(g) \rightarrow -(C-C(O)-C^*(O))_{n-} + NO \quad (15)$$

$$-(C-C(O)-C^*(O))_{n-} \rightarrow -(C-C^*)_{n-1-} + CO_2 \quad (16)$$

In the case of the NO, where N_2 and CO_2 should be the detected products, it would be by this way:

$$-(C-C^*)_{n-} + NO(g) \rightarrow -(C-C^*)_{n}-(O) + N^* \quad (17)$$

$$-(C-C^*)_{n}-(O) + NO(g) \rightarrow -(C-C(O)-C^*(O))_{n-} + N^* \quad (18)$$

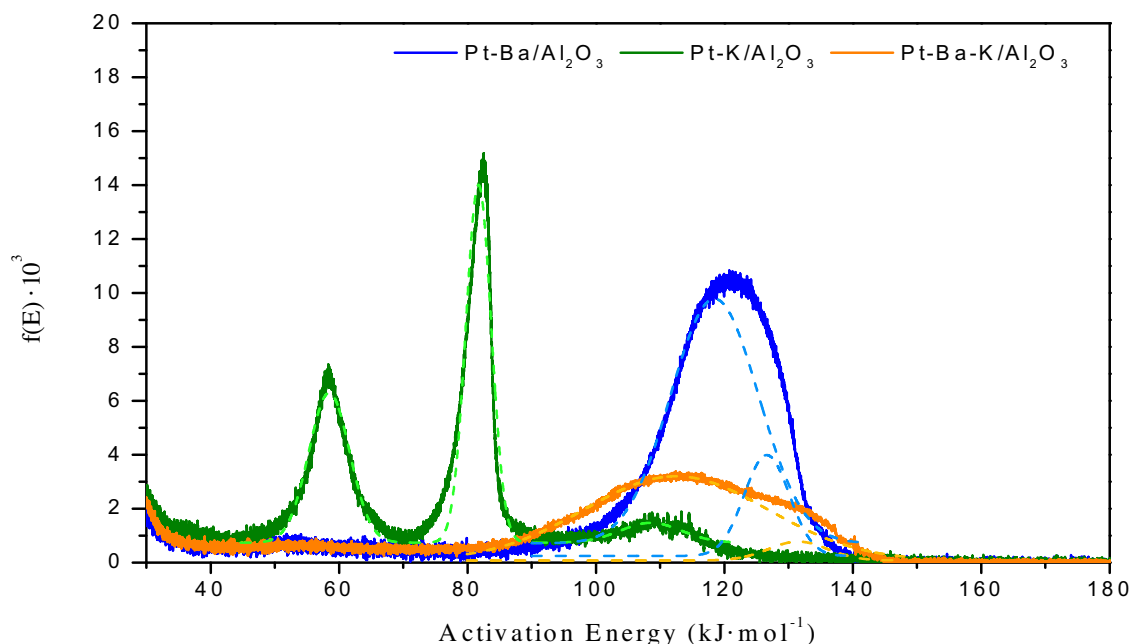$$-(C-C(O)-C^*(O))_{n-} \rightarrow -(C-C^*)_{n-1-} + CO_2 \quad (19)$$

Fig. 4. Distribution functions of activation energy and deconvolution of signals for the catalysed soot removal process in the presence of 3% of O_2 in He.
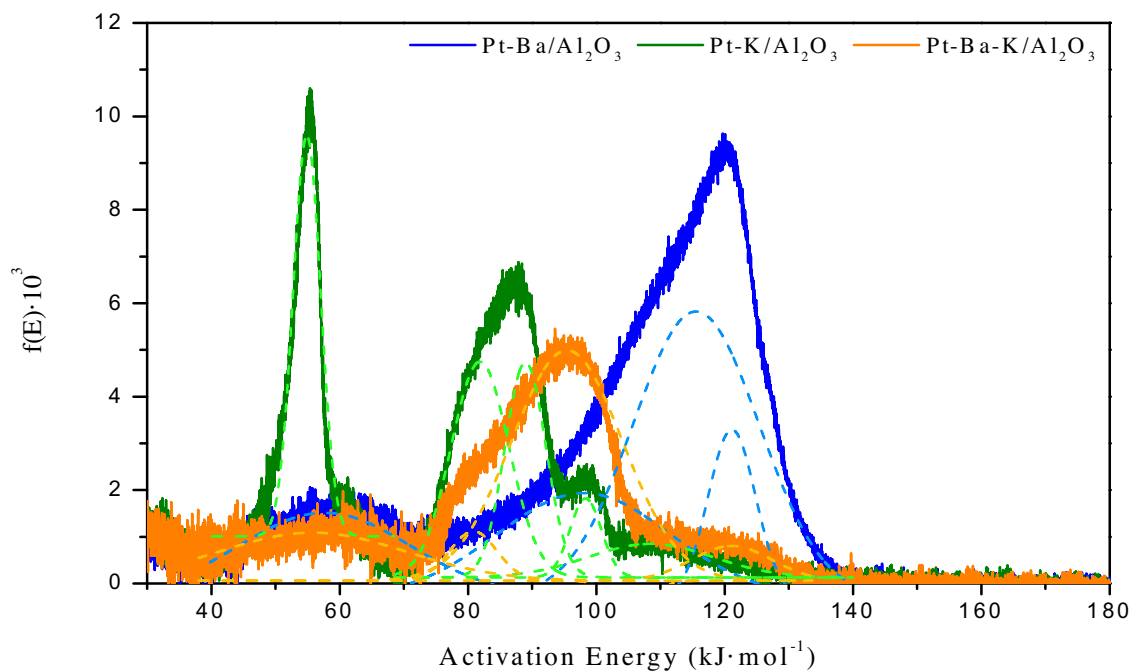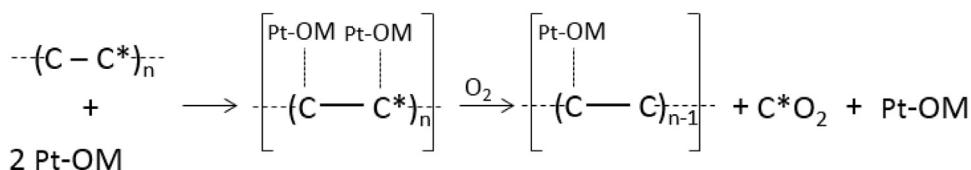

Fig. 5. Distribution functions of activation energy and deconvolution of signals for the catalysed soot removal process in the presence of 1000 ppm of NO and 3% of O_2 in He.

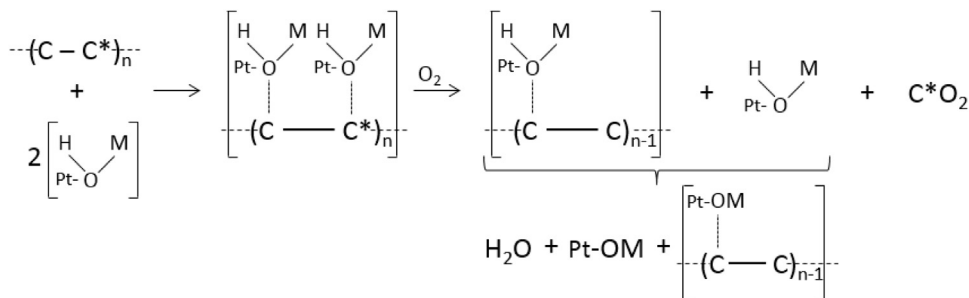$$N^* + N^* \rightarrow N_2 \qquad (20)$$

This first route was apparently more plausible in concordance with the results obtained by mass spectrometry (data not shown), where it was observed an increase of the NO signal in the temperature range between 823 and 973 K with a simultaneous CO_2 production besides the additional CO_2 formation that is extended up to 1023 K; indicating that the removal process occurs in greater proportion by the influence of the NO_2, due to its higher oxidizing power according to the equilibrium: $NO + O_2 \leftrightarrow NO_2$. It was also reported that the soot properties, including microstructure, elemental analysis, ash content and ash composition, determine its reactivity toward oxidation with synthetic air and NO_x [3,29,57,58].

The distribution functions for catalyzed soot removal process in an oxygen atmosphere and the deconvolution of signals are shown in Fig. 4. For the PtBa/Al_2O_3 with a LNT-catalyst standard formulation, the distribution function calculated was a *quasi*-symmetric curve with a maximum localized close to 120 kJ mol^{-1}. However, the deconvolution showed that this oxidation process is a series of coupled processes due to two activation energies values were registered at 117 and 128 kJ mol^{-1}; associated with O_2-ads catalyst and the O_2 gas phase contributions, respectively.

A totally different situation is observed over PtK/Al_2O_3 catalyst, where the soot elimination occurs in three steps, as can be observed by the maxima in the distribution curve obtained. Three

Scheme 2. Mechanism of soot combustion under O_2 atmosphere over alkaline-earth metal.

Scheme 3. Mechanism of soot combustion under O_2 atmosphere over alkaline metal.

values of activation energy at 60, 85 and 110 kJ mol^{-1} are noteworthy, indicating that exist several coupled processes in the soot removal. The first activation energy value clearly corresponds to the removal of water and is associated with water physisorbed in the catalyst (water signal below 400 K accompanied by the weight loss in the TG-curve) with 60 kJ mol^{-1} that coincides with the water condensation heat value. The second value of the activation energy, with the highest frequency value, may be associated with a second process in which is mainly involved the structural or chemisorbed surface water by the presence of potassium in the formulation and registering a parallel CO_2 formation during this step. It has also been suggested that K has high mobility and is able to keep in contact with the soot [6,11,12,14,59], which enhances the combustion of soot remote from the active sites (propagation of the combustion). The third activation energy, with a broader signal with the lowest frequency value, is very close to those calculated for PtBa/Al$_2$O$_3$ catalyst, indicating that the final step should be related to the soot assisted combustion, where the O_2 adsorbed species might be involved. For the trimetallic catalyst, PtBaK/Al$_2$O$_3$, a very broad and non-symmetrical distribution curve was obtained and its deconvolution provides two values of activation energy at 110 and 130 kJ mol^{-1}, which would indicate the participation of the O_2-adsorbed on mixed-alkaline surface sites and the molecular O_2 presents in gas phase in the removal of soot. This further indicates that the behavior in the elimination of soot is closer to the bimetallic PtBa/Al$_2$O$_3$ catalyst, probably related to the lower K/Ba ratio and the similarity in the Pt$^{\circ}$/Pt$_{ox}$ relationship.

Up to now we assume that the oxidation of soot takes place through the participation of different metal centers that involve different activated steps and, although to less extent, by reaction with molecular oxygen. This latter route is more common for low contact mode soot elimination [32] and the uncatalyzed combustion process. Taking in consideration these calculated values of activation energy for the catalytic soot removal, it is assumed that the alkaline (-earth) oxide and in particular the Pt—O—M centers or Pt—O—M—OH sites (where M represents Ba, K or Ba + K) are involved in some of the steps of soot elimination by oxygen (see Schemes 2 and 3). The role of alkali compounds in the oxygen-transfer mechanism is ascribed to their electron-donating effect which increases the local electron density of neighboring C-sites promoting their affinity for binding an oxygen atom. As a consequence, this leads to the substantial weakening of the carbon bonds and thus promotes the carbon shortening chain process.

In Fig. 5 the function of distribution of activation energy in NO + O_2 atmosphere is shown. For the PtBa/Al$_2$O$_3$, the function takes a non-evident symmetrical distribution, with a similar maximum of frequency value at 120 kJ mol^{-1}, besides an additional weak contribution close to 60 kJ mol^{-1}. However, the deconvolution of the major frequency contribution process, evidenced the contribution of two sequential reactions with a shift to lower activation energy, close to 105 and 118 kJ mol^{-1}, with respect to that found for the same catalyst in O_2-atmosphere. It is known that this LNT-catalyst is able to oxidize and store a high amount of NO$_x$-species, in nitrite and nitrate forms. So, the shifting to lower activation energy and the higher frequency values appreciated in the distribution function were justified by the intervention of more reactive oxidant species as the NO$_x$-adsorbed onto catalyst and by the more oxidant atmosphere; those were found for adsorbed catalyst species and the oxygen in the gas-phase, in the experiments performed in O_2 atmosphere.

Over PtK/Al$_2$O$_3$ catalyst it is also possible to appreciate a significant change in the symmetry of signals and the occurrence of different reactions for the distribution function when the soot elimination was performed in NO + O_2 atmosphere. The maximum of frequency value $f(E)$ was found for an activation energy value close to 56 kJ mol^{-1} and the minimal for 108 kJ mol^{-1}. Besides, a complex signal is observed whose deconvolution resulted in kinetic parameter values of 78, 90 and 98 kJ mol^{-1}. In NO + O_2 atmosphere over K-containing catalyst it clearly evidences that soot removal is faster than in the case of Ba-containing catalyst. This might be associated with more effective surface species that should be involved during the soot elimination process compared to PtBa/Al$_2$O$_3$ catalyst. Since water production was higher than the production of CO_2 during the removal of soot with this catalyst, the involved reactions having different values of activation energies should be related to the intervention of the potassium surface OH-groups, the stored nitrate species and the surface oxide species in the oxidation of soot, respectively.

For the PtBaK/Al$_2$O$_3$ catalyst, the maximum frequency value is evidenced by the very broad and non-symmetrical distribution curve obtained, with a relative activation energy value centered at 98 kJ mol^{-1}, in addition to other two reactions with less occurrence at 60 and 120 kJ mol^{-1}. These latter were associated with water release and the participation of the NO$_x$ in the gas-phase in the soot removal by assisted combustion, respectively. The deconvolution of the main contribution evidences the participation of two

Table 3
Summary of soot removal processes in O_2 atmosphere.

T (K)	Ea (kJ mol^{-1})	Soot	Pt-Ba/Al$_2$O$_3$	Pt-K/Al$_2$O$_3$	Pt-Ba-K/Al$_2$O$_3$
473–673	45–70	–	Physisorbed H$_2$O desorption	Physisorbed and Chemisorbed H$_2$O desorption	
673–773	70–90	–	–	C + Pt—OH—M	
873–973	105–120	C + O$_2$ (g)		C + Pt—O—M	
973–1073	120–140			C + O$_2$ (g)	

Table 4
Summary of soot removal processes in NO + O$_2$ atmosphere.

T (K)	Ea (kJ mol^{-1})	Soot	Pt-Ba/Al$_2$O$_3$	Pt-K/Al$_2$O$_3$	Pt-Ba-K/Al$_2$O$_3$
473–673	45–70	–	Physisorbed H$_2$O desorption	Physisorbed and Chemisorbed H$_2$O desorption	
673–773	70–90	–	–	C + Pt—OH—M	
773–873	90–105	–		C + NO$_x$ (ads)	
873–973	105–120	C + NO$_x$ (g)		C + Pt—O—M	
973–1073	120–140			C + O$_2$ (g)	

parallel reactions with a shift to lower activation energy close to 82 and 95 kJ mol^{-1}, which would be related to the participation of the nitrate-stored species and the Oads centers in the soot elimination process at lower temperature.

The reactivity of LNT-catalysts towards soot oxidation, under non-isothermal conditions and different environments, points out that the alkaline and alkaline-earth-containing catalysts exhibit a significant higher activity in the soot removal than Pt/Al$_2$O$_3$ catalyst or even themselves free-Pt using the same alumina support. Besides, a more oxidizing (NO + O$_2$) atmosphere as diesel gas-off combustion environment with the presence of NO$_2$ which is dominant at temperatures in the range of 423–673 K, as was proposed by Jelles et al. [43], facilitates the soot oxidation to CO$_2$ at lower temperature [8,49] and subsequently the lowering the activation energy values, even for the uncatalyzed process.

Unlike what occurs for the PtBa/Al$_2$O$_3$ catalyst, the presence of a more hydrated and higher hydroxylated surface is observed over PtK/Al$_2$O$_3$ and also, although less-evident, for PtBaK/Al$_2$O$_3$ catalysts. For the PtBa catalyst, the O$_2$-atmosphere promotes the soot elimination at lower temperature by partial gasification of carbon with CO$_2$ as main product. The water formation that happens at temperatures close to 400 K and with energy of activation value between 57–60 kJ mol^{-1} is due to released physisorbed water for LNT-catalysts. For the K-containing catalysts, the second water contribution evidenced at temperatures below 600 K with an estimated activation energy value close to 80 kJ mol^{-1} in both atmospheres and with CO$_2$ production is associated with the soot elimination by intervention of OH groups. A parallel and additive way, imperceptible in absence of NO, has been noted as additional reaction in the soot elimination process; which depends on the formulation of catalysts, with activation energy values close to 85, 95 and 105 kJ mol^{-1} for PtK, PtBaK and PtBa catalysts, respectively. The differences between these values are associated with the stability of the different nitrates species stored onto catalysts. So that, the signals in the distribution function are justified in agreement with the products registered by mass spectrometry. Additional experiments were performed (data not shown) in which the decomposition of different types of nitrates was carried out to check the temperature and the activation energy values corresponding to the release of NO$_x$. So the N$_2$ and CO$_2$ produced by reaction between soot and the adsorbed nitrates on the catalyst surface [12,59], would suggest that the route for the soot elimination might proceed in a manner analogous to that described by Shangguan et al. [3]

$$-(C—C^*)_{n-} + NO_{ads} \rightarrow -(C—C^*)_n-(NO) \qquad (21)$$

$$-(C—C^*)_n-NO + NO_{ads} \rightarrow -(C—C^*)_{n-1-} + CO_2(g) + N_2(g) \qquad (22)$$

where the adsorbed NO$_x$ attack the most accessible carbon producing CO$_2$ and nitrogen and the shortening of the carbon chain.

Although soot oxidation in diesel engine has been investigated in several studies prior to this work, the kinetic data for soot removal process have been further analyzed considering a network of first-order reactions represented by the activation energy and the frequency factor. So, the influence of the gas phase on reactivity and the composition of LNT-catalysts on the decoupling processes that occurred and the kinetic parameters are summarized on the Tables 3 and 4.

For the soot model used in this contribution, although it is well-known that the soot nanostructure which depends on the fuel and the engine performances plays an important role in the overall activity, the differences in the temperature ranges and the activation energy values are reported, and these are linked with the highest frequency value of the parallel and decoupled processes. It is generally accepted that the NO + O$_2$ environment with respect to O$_2$ atmosphere enhances the oxidation of soot, but the effect of induced reactivity should also be related to the characteristics and functionalization of the catalyst surfaces by the modification of the frequency values registered. Apart from the gas phase contribution on the soot oxidation by molecular O$_2$ and NO$_x$(g), the interaction of carbon-chain with the active centers of catalyst surface should modify the local electron density of the carbon sites with a weakening of C—C bonds in the carbon-chain due to the electro-donating by the electropositive character of Pt—O—M and Pt—OH—M (M = K, Ba or Ba-K) centers that favours the oxygen-transfer mechanism and subsequently the shortening of the carbon-chain. Thus hydroxylated centers associated with alkaline nature, promote the partial removal of the carbon by gasification process at the lowest temperature range. The O—M centers, based in the intermediate O-containing species detected, also contribute to the shortening of carbon chain but a higher temperature range. Besides, the NO$_x$-adsorbed (NO$_x$-ads) species, whose proportion in NO$_x$ atmosphere is very much considerable for these DPNR-catalysts, improve the relative contribution of reactivity lowering the temperature range of overall process and enhance the soot removal rate by oxidation.

The proposed mechanisms schemes provide information of the primary products (CO, CO$_2$ and H$_2$O) and the process that occurs with a higher frequency, for the non- and catalytic process condition and are in agreement with the kinetic parameters calculated throughout the function of distribution of activation energy, which permits the intrinsic reactivity analysis by identification of the sequential steps that occur in the complex catalytic soot removal process.

The overall process was analyzed based on a model in which the reactions consist of many first-order reactions each of which has different frequency factor besides different energy activation. The difference in the activation energies was represented by a distribu-

tion curve that was obtained by analysis of the thermogravimetric curves measured at a constant heating in a different atmospheres; in the currently case of the intrinsic analysis of soot removal over LNT-catalysts. The model is expected to be applicable to the analysis of the decoupled complex reactions.

4. Conclusions

The soot removal process over LNT catalysts was analyzed on the basis of a model that the soot elimination consists of a set of first-order reactions, which have different activation energy and frequency factor. The frequency factor was correlated by a function of the activation energy and the differences in the activation energy values were represented by the distribution curves obtained from the analysis of the TG-curves. This approach permits to describe the intrinsic reactivity through the kinetic parameters and the distribution of products. A sequential process was described, where reactions were differenced and individualized based on kinetic parameters and the role of the different species involved in the complex process of eliminating soot was identified even in different atmospheres.

Alkali and alkali-earth metals have a beneficial significant effect on the elimination process by intervention of hydroxylated (Pt—OH—M) surfaces and the oxygen-containing (Pt-O-M) centers, respectively. In addition, the reaction atmosphere modifies the route, by add-contribution of reactions between the carbon and the adsorbed NO_x and/or NO_2 in gas phase completing the soot removal at lower temperatures.

References

[1] I.S. Pieta, M. García-Diéguez, C. Herrera, M. a. Larrubia, L.J. Alemany, In situ DRIFT-TRM study of simultaneous NO_x and soot removal over Pt-Ba and Pt-K NSR catalysts, J. Catal. 270 (2010) 256–267, http://dx.doi.org/10.1016/j.jcat.2010.01.003.

[2] F. Dai, M. Meng, Y. Zha, Z. Li, T. Hu, Y. Xie, et al., Performance of Ce substituted hydrotalcite-derived mixed oxide catalysts Co2.5Mg0.5Al1-X%Ce$_x$%O used for soot combustion and simultaneous NO_x-soot removal, Fuel Process. Technol. 104 (2012) 43–49, http://dx.doi.org/10.1016/j.fuproc.2012.07.002.

[3] W.F. Shangguan, Y. Teraoka, S. Kagawa, Kinetics of soot-O2, soot-NO and soot-O2NO reactions over spinel-type CuFe2O4 catalyst, Appl. Catal. B: Environ. 12 (1997) 237–247.

[4] Q. Shen, G. Lu, C. Du, Y. Guo, Y. Wang, Y. Guo, et al., Role and reduction of NO_x in the catalytic combustion of soot over iron-ceria mixed oxide catalyst, Chem. Eng. J. 218 (2013) 164–172, http://dx.doi.org/10.1016/j.cej.2012.12.010.

[5] I. Atribak, I. Such-Basáñez, a. Bueno-López, a. García, Comparison of the catalytic activity of MO2 (M = Ti, Zr, Ce) for soot oxidation under NO_x/O2, J. Catal. 250 (2007) 75–84, http://dx.doi.org/10.1016/j.jcat.2007.05.015.

[6] M.a. Peralta, M.S. Zanuttini, M.a. Ulla, C.a. Querini, Diesel soot and NO_x abatement on K/La2O3 catalyst: influence of K precursor on soot combustion, Appl. Catal. A: Gen. 399 (2011) 161–171, http://dx.doi.org/10.1016/j.apcata.2011.03.046.

[7] C.-B. Lim, H. Kusaba, H. Einaga, Y. Teraoka, Catalytic performance of supported precious metal catalysts for the combustion of diesel particulate matter, Catal. Today 175 (2011) 106–111, http://dx.doi.org/10.1016/j.cattod.2011.03.062.

[8] R. Matarrese, L. Castoldi, L. Lietti, P. Forzatti, Soot combustion: reactivity of alkaline and alkaline earth metal oxides in full contact with soot, Catal. Today 136 (2008) 11–17, http://dx.doi.org/10.1016/j.cattod.2008.03.022.

[9] R. Matarrese, L. Castoldi, L. Lietti, Reaction between soot and stored NO_x over K-based LNT catalysts investigated by temperature programmed methods and labeling isotopic experiments, Catal. Today 197 (2012) 228–235, http://dx.doi.org/10.1016/j.cattod.2012.07.046.

[10] Z. Wang, Q. Li, L. Wang, W. Shangguan, Simultaneous catalytic removal of NO_x and soot particulates over CuMgAl hydrotalcites derived mixed metal oxides, Appl. Clay Sci. 55 (2012) 125–130, http://dx.doi.org/10.1016/j.clay.2011.11.003.

[11] Q. Li, M. Meng, F. Dai, Y. Zha, Y. Xie, T. Hu, et al., Multifunctional hydrotalcite-derived K/MnMgAlO catalysts used for soot combustion, NO_x

[12] V.G. Milt, C.A. Querini, E.E. Miró, M.A. Ulla, Abatement of diesel exhaust pollutants: NO_x adsorption on Co,Ba,K/CeO2 catalysts, J. Catal. 220 (2003) 424–432, http://dx.doi.org/10.1016/S0021-9517(03)00285-9.

[13] Y. Wei, Z. Zhao, J. Liu, S. Liu, C. Xu, A. Duan, et al., Multifunctional catalysts of three-dimensionally ordered macroporous oxide-supported Au@Pt core–shell nanoparticles with high catalytic activity and stability for soot oxidation, J. Catal. 317 (2014) 62–74, http://dx.doi.org/10.1016/j.jcat.2014.05.014.

[14] K. Krishna, M. Makkee, Soot oxidation over NO_x storage catalysts: activity and deactivation, Catal. Today 114 (2006) 48–56, http://dx.doi.org/10.1016/j.cattod.2006.02.009.

[15] M.E. Gálvez, S. Ascaso, I. Tobías, R. Moliner, M.J. Lázaro, Catalytic filters for the simultaneous removal of soot and NO_x: influence of the alumina precursor on monolith washcoating and catalytic activity, Catal. Today 191 (2012) 96–105, http://dx.doi.org/10.1016/j.cattod.2011.12.012.

[16] L. Xu, R.W. McCabe, LNT + in situ SCR catalyst system for diesel emissions control, Catal. Today 184 (2012) 83–94, http://dx.doi.org/10.1016/j.cattod.2011.12.005.

[17] B. Pereda-Ayo, D. Duraiswami, J.R. González-Velasco, Control of NO_x storage and reduction in NSR bed for designing combined NSR–SCR systems, Catal. Today 172 (2011) 66–72, http://dx.doi.org/10.1016/j.cattod.2011.01.043.

[18] U. De La Torre, B. Pereda-Ayo, J.R. González-Velasco, Cu-zeolite NH3-SCR catalysts for NO_x removal in the combined NSR–SCR technology, Chem. Eng. J. 207–208 (2012) 10–17, http://dx.doi.org/10.1016/j.cej.2012.06.092.

[19] L. Castoldi, R. Bonzi, L. Lietti, P. Forzatti, S. Morandi, G. Ghiotti, et al., Catalytic behaviour of hybrid LNT/SCR systems: reactivity and in situ FTIR study, J. Catal. 282 (2011) 128–144, http://dx.doi.org/10.1016/j.jcat.2011.06.002.

[20] I. Nova, L. Lietti, P. Forzatti, Mechanistic aspects of the reduction of stored NO_x over Pt–Ba/Al2O3 lean NO_x trap systems, Catal. Today 136 (2008) 128–135, http://dx.doi.org/10.1016/j.cattod.2008.01.006.

[21] U. Elizundia, D. Duraiswami, B. Pereda-Ayo, R. López-Fonseca, J.R. González-Velasco, Controlling the selectivity to N2O over Pt/Ba/Al2O3 NO_x storage/reduction catalysts, Catal. Today 176 (2011) 324–327, http://dx.doi.org/10.1016/j.cattod.2010.11.075.

[22] I. Malpartida, M.A. Larrubia Vargas, L.J. Alemany, E. Finocchio, G. Busca, Pt–Ba–Al2O3 for NO_x storage and reduction: characterization of the dispersed species, Appl. Catal. B: Environ. 80 (2008) 214–225, http://dx.doi.org/10.1016/j.apcatb.2007.11.035.

[23] L. Castoldi, N. Artioli, R. Matarrese, L. Lietti, P. Forzatti, Study of DPNR catalysts for combined soot oxidation and NO_x reduction, Catal. Today 157 (2010) 384–389, http://dx.doi.org/10.1016/j.cattod.2010.03.022.

[24] J.Y. Luo, W.S. Epling, New insights into the promoting effect of H2O on a model Pt/Ba/Al2O3 NSR catalyst, Appl. Catal. B: Environ. 97 (2010) 236–247, http://dx.doi.org/10.1016/j.apcatb.2010.04.007.

[25] S. Ye, Y.H. Yap, S.T. Kolaczkowski, K. Robinson, D. Lukyanov, Catalyst light-off experiments on a diesel oxidation catalyst connected to a diesel engine-methodology and techniques, Chem. Eng. Res. Des. 90 (2012) 834–845, http://dx.doi.org/10.1016/j.cherd.2011.10.003.

[26] V. Rico Pérez, A. Bueno-López, Catalytic regeneration of diesel particulate filters: comparison of Pt and CePr active phases, Chem. Eng. J. 279 (2015) 79–85, http://dx.doi.org/10.1016/j.cej.2015.05.004.

[27] C. Lee, J.-I. Park, Y.-G. Shul, H. Einaga, Y. Teraoka, Ag supported on electrospun macro-structure CeO2 fibrous mats for diesel soot oxidation, Appl. Catal. B: Environ. 174–175 (2015) 185–192, http://dx.doi.org/10.1016/j.apcatb.2015.03.008.

[28] M. Schejbal, M. Marek, M. Kubíček, P. Kočí, Modelling of diesel filters for particulates removal, Chem. Eng. J. 154 (2009) 219–230, http://dx.doi.org/10.1016/j.cej.2009.04.056.

[29] R. López-Fonseca, U. Elizundia, I. Landa, M.A. Gutiérrez-Ortiz, J.R. González-Velasco, Kinetic analysis of non-catalytic and Mn-catalysed combustion of diesel soot surrogates, Appl. Catal. B: Environ. 61 (2005) 150–158, http://dx.doi.org/10.1016/j.apcatb.2005.04.016.

[30] X. Guo, M. Meng, F. Dai, Q. Li, Z. Zhang, Z. Jiang, et al., NOx-assisted soot combustion over dually substituted perovskite catalysts La1-xKxCo1-yPdyO3-ı, Appl. Catal. B: Environ. 142–143 (2013) 278–289, http://dx.doi.org/10.1016/j.apcatb.2013.05.036.

[31] L. Castoldi, R. Matarrese, L. Lietti, P. Forzatti, Intrinsic reactivity of alkaline and alkaline-earth metal oxide catalysts for oxidation of soot, Appl. Catal. B: Environ. 90 (2009) 278–285, http://dx.doi.org/10.1016/j.apcatb.2009.03.022.

[32] H. Shimokawa, Y. Kurihara, H. Kusaba, Y. Einaga, Y. Teraoka, Comparison of catalytic performance of Ag- and K-based catalysts for diesel soot combustion, Catal. Today 185 (2012) 99–103, http://dx.doi.org/10.1016/j.cattod.2011.10.030.

[33] A. Yezerets, N.W. Currier, D.H. Kim, H.A. Eadler, W.S. Epling, C.H.F. Peden, Differential kinetic analysis of diesel particulate matter (soot) oxidation by oxygen using a step-response technique, Appl. Catal. B: Environ. 61 (2005) 120–129, http://dx.doi.org/10.1016/j.apcatb.2005.04.014.

[34] N. Artioli, R. Matarrese, L. Castoldi, L. Lietti, P. Forzatti, Effect of soot on the storage-reduction performances of PtBa/Al2O3 LNT catalyst, Catal. Today 169 (2011) 36–44, http://dx.doi.org/10.1016/j.cattod.2010.10.062.

[35] I. Atribak, a. Bueno-López, a. García-García, Uncatalysed and catalysed soot combustion under NO_x + O2: Real diesel versus model soots, Combust. Flame. 157 (2010) 2086–2094, http://dx.doi.org/10.1016/j.combustflame.2010.04.018.

[36] A. Setiabudi, M. Makkee, J.A. Moulijn, An optimal NO_x assisted abatement of diesel soot in an advanced catalytic filter design, Appl. Catal. B: Environ. 42 (2003) 35–45, http://dx.doi.org/10.1016/S0926-3373(02)00213-8.

[37] A. Fritz, V. Pitchon, The current state of research on automotive lean NO_x catalysis, Appl. Catal. B: Environ. 13 (1997) 1–25, http://dx.doi.org/10.1016/S0926-3373(96)00102-6.

[38] Z. Li, M. Meng, Q. Li, Y. Xie, T. Hu, J. Zhang, Fe-substituted nanometric La0.9K0.1Co1-xFe$_x$O$_3$-d perovskite catalysts used for soot combustion, NO_x storage and simultaneous catalytic removal of soot and NO_x, Chem. Eng. J. 164 (2010) 98–105, http://dx.doi.org/10.1016/j.cej.2010.08.036.

[39] H. Lin, Y. Li, W. Shangguan, Z. Huang, Soot oxidation and NO_x reduction over BaAl2O4 catalyst, Combust. Flame 156 (2009) 2063–2070, http://dx.doi.org/10.1016/j.combustflame.2009.08.006.

[40] Q. Li, M. Meng, N. Tsubaki, X. Li, Z. Li, Y. Xie, et al., Performance of K-promoted hydrotalcite-derived CoMgAlO catalysts used for soot combustion, NO_x storage and simultaneous soot-NO_x removal, Appl. Catal. B: Environ. 91 (2009) 406–415, http://dx.doi.org/10.1016/j.cej.2012.01.009.

[41] L. Castoldi, R. Matarrese, L. Lietti, P. Forzatti, Simultaneous removal of NO_x and soot on Pt–Ba/Al2O3 NSR catalysts, Appl. Catal. B: Environ. 64 (2006) 25–34, http://dx.doi.org/10.1016/j.apcatb.2005.10.015.

[42] M. Cortés-Reyes, I.S. Pieta, M.C. Herrera, M.A. Larrubia, L.J. Alemany, In situ TG-MS study of simultaneous NOx and soot removal over LNT, APCATA-D-00572.

[43] S.J. Jelles, R.R. Krul, M. Makkee, J.A. Moulijn, The influence of NO_x on the oxidation of metal activated diesel soot, Catal. Today 53 (1999) 623–630, http://dx.doi.org/10.1016/S0920-5861(99)00150-9.

[44] A. Setiabudi, M. Makkee, J.A. Moulijn, The role of NO_2 and O_2 in the accelerated combustion of soot in diesel exhaust gases, Appl. Catal. B: Environ. 50 (2004) 185–194, http://dx.doi.org/10.1016/j.apcatb.2004.01.004.

[45] J.P.A. Neeft, M. Makkee, J.A. Moulijn, Catalysts for the oxidation of soot from diesel exhaust gases. I. An exploratory study, Appl. Catal. B: Environ. 8 (1996) 57–78, http://dx.doi.org/10.1016/0926-3373(95)00057-7.

[46] D. Uner, M.K. Demirkol, B. Dernaika, A novel catalyst for diesel soot oxidation, Appl. Catal. B: Environ. 61 (2005) 334–345, http://dx.doi.org/10.1016/j.apcatb.2005.05.011.

[47] R. López-Fonseca, I. Landa, U. Elizundia, M.A. Gutiérrez-Ortiz, J.R. González-Velasco, Thermokinetic modeling of the combustion of carbonaceous particulate matter, Combust. Flame 144 (2006) 398–406, http://dx.doi.org/10.1016/j.combustflame.2005.08.012.

[48] B.R. Stanmore, J.F. Brilhac, P. Gilot, The oxidation of soot: a review of experiments, mechanisms and models, Carbon N. Y. 39 (2001) 2247–2268.

[49] J.-O. Müller, B. Frank, R.E. Jentoft, R. Schlögl, D.S. Su, The oxidation of soot particulate in the presence of NO2, Catal. Today 191 (2012) 106–111, http://dx.doi.org/10.1016/j.cattod.2012.03.010.

[50] I.S. Pieta, M. García-Diéguez, M.A. Larrubia, L.J. Alemany, W.S. Epling, Sn-modified NO_x storage/reduction catalysts, Catal. Today 207 (2013) 200–211, http://dx.doi.org/10.1016/j.cattod.2012.04.016.

[51] N. Nejar, M. Makkee, M.J. Illán-Gómez, Catalytic removal of NO_x and soot from diesel exhaust: oxidation behaviour of carbon materials used as model soot, Appl. Catal. B: Environ. 75 (2007) 11–16, http://dx.doi.org/10.1016/j.apcatb.2007.03.009.

[52] R. Buchel, R. Strobel, F. Krumeich, A. Baiker, S.E. Pratsinis, Influence of Pt location on BaCO3 or Al$_2$O$_3$ during NO_x storage reduction, J. Catal. 261 (2009) 201–207, http://dx.doi.org/10.1016/j.jcat.2008.11.016.

[53] D.B. Anthony, J.B. Howard, H.C. Hottel, H.P. Meissner, Rapid devolatilization and hydrogasification of bituminous coal, Fuel 55 (1976) 121–128, http://dx.doi.org/10.1016/0016-2361(76)90008-9.

[54] V. Vand, A theory of the irreversible electrical resistance changes of metallic films evaporated in vacuum, Proc. Phys. Soc. 55 (1943) 222, http://dx.doi.org/10.1088/0959-5309/55/3/308.

[55] K. Hashimoto, K. Miura, T. Watanabe, Kinetics of thermal regeneration reaction of activated carbons used in waste water treatment, AIChE J. (1982).

[56] R. Brukh, S. Mitra, Kinetics of carbon nanotube oxidation, J. Mater. Chem. 17 (2007) 619–623, http://dx.doi.org/10.1039/b60921g.

[57] R. López-Fonseca, I. Landa, U. Elizundia, M.A. Gutiérrez-Ortiz, J.R. González-Velasco, A kinetic study of the combustion of porous synthetic soot, Chem. Eng. J. 129 (2007) 41–49, http://dx.doi.org/10.1016/j.cej.2006.10.029.

[58] B. Dernaika, D. Uner, A simplified approach to determine the activation energies of uncatalyzed and catalyzed combustion of soot, Appl. Catal. B: Environ. 40 (2003) 219–229.

[59] S. Ascaso, M.E. Gálvez, P. Da Costa, R. Moliner, M.J. Lázaro, On the influence of the alumina precursor in Fe-K/Al$_2$O$_3$ structured catalysts for the simultaneous removal of soot and NO_x: from surface properties to reaction mechanism, C. R. Chim. 17 (2014) 681–686, http://dx.doi.org/10.1016/j.crci.2013.08.001.